AIMS Geosciences

http://www.aimspress.com/journal/geosciences/

AIMS Geosciences, 3(1): 67-90
DOI: 10.3934/geosci.2017.1.67
Received: 22 October 2016
Accepted: 23 January 2017
Published: 25 February 2017

Research article

Effect of Hydrological Properties on the Energy Shares of Reflected Waves at the Surface of a Partially Saturated Porous Solid

Mahabir Barak[1], **Manjeet Kumari**[1,*] **and Manjeet Kumar**[2]

[1] Dept. of Mathematics, Indira Gandhi University Meerpur, India-122503
[2] Dept. of Mathematics, C.M.R.J Govt. College, Ellenabad, India-125102

[*] **Correspondence:** manjeet.aryan17@gmail.com; Tel: +919068793155

Abstract: In the present study, the reflection of inhomogeneous waves is investigated at the stress-free plane surface based on multiphase poroelasticity theory. The porous medium is considered as dissipative due to the presence of viscosity in pores fluid. Four inhomogeneous (i.e. different direction of propagation and attenuation) reflected waves (three longitudinal and one shear) exists due to an incident wave. By using the appropriate boundary conditions, closed-form analytical expressions for the reflection coefficients are derived at the stress-free surface. These reflection coefficients are used to drive the analytical expressions for the energy shares of various reflected inhomogeneous waves. In mathematical framework, the conservation of incident energy is confirmed by considering an interaction energy between two dissimilar waves. It validates that the numerical calculations are analytically correct. Finally, a numerical example is considered to study the effects of viscous cross-coupling, porosity, saturation of gas, pore-characteristics and wave frequency on the energy shares of various reflected inhomogeneous waves and depicted graphically.

Keywords: viscous cross-coupling; partially saturated porous solid; immiscible pore-fluids; inhomogeneous wave; reflection coefficients

1. Introduction

The phenomenon of wave propagation in multiphase poroelasticity theory is appealing extensive attention due to its importance in large number of practical applications in the fields of seismology, geophysics, rock mechanics, soil mechanics and hydrogeology. Biot [14] was the first who introduce the equations of motion for the propagation of elastic waves in a porous solid saturated with single fluid. He found that three (two longitudinal and one shear) waves exist in such a porous medium. In comparison to the porous medium saturated with single fluid, the studies of porous media saturated by multi-fluids are rare. For more realistic interpretations of elastic waves propagation in porous me-

dia demand an accurate and developed mathematical theory. An approach, based on mixture concept, Brutsaert [5] was the first who extended Biot's theory as Mixture theory to includes the effects of two immiscible pore fluids on the behaviour of elastic waves propagation. Mixture theory, generally, developed for two-fluid system, was further improved and generalised by many authors (Brutsaert and Luthin [6]; Bedford and Drumheller [7]; Garg and Nayfeh [8]; Berryman et al. [9]; Santos et al. [10,11]; Corapcioglu and Tuncay [12]; Tuncay and Corapcioglu [13]; Wei and Muraleethara [14,15]; Hanyga [16]; Lu and Hanyga [17]; Lo [18]; Lo et al. [1921]). In multiphase poroelasticity theory, the solution of coupled differential equations of motion showed that four (three longitudinal and one shear) mode of elastic waves exist. Based on the above mentioned models, a study of reflection of plane harmonic waves at the stress-free surface of porous solid have been carried out by some researchers e.g. Sharma and Kumar [22]; Kumar and Kumari [23]; Sharma [24]; Sharma[25]; Tomer and Goyal [26]. A latest book by Carcione [27] is referred for relevant references and detailed procedures. In all the above mentioned hydrologic models of subsurface multiphase flow, the effect of viscous resistance due to relative velocity between two adjacent fluids on elastic waves behavior in unsaturated porous media still remains ignored. A recent mathematical model 'based on continuum mixture theory' presented by Lo et al. [28] incorporated the viscous cross-coupling between two immiscible pore fluids. Thus, all the above mentioned models can be derived as the special case of this model. Further, in case of single fluid in medium, this model reduced to Biot [1,2] theory. To account the viscous resistance, they first generalised the equations of motion proposed by Lo et al. [19]. Next, they derived the dispersion relations, which physically shows the existence of four (three longitudinal and one shear) waves in such a medium. At different frequency and water saturation level, the essence of viscous cross coupling on the phase speed and attenuation coefficient of these four elastic waves is analysed for Columbia fine sandy loam containing an gas-water mixture.Keeping the importance of viscous cross-coupling in mind, in this work, we have extended the work of Lo et al. [28]. Present study considers the reflection of inhomogeneous waves at the stress-free plane surface. The methodology is analogous to that presented in Sharma [28]. Firstly, the mathematical model developed by Lo et al. [28] is solved for the propagation of three compressional waves and lone transverse wave after that definition and suitable boundary conditions for the problem are described. By using the appropriate boundary conditions, the closed-form analytical expressions for the reflection coefficients are derived at the stress-free surface. The analytical expressions for the energy shares of various reflected inhomogeneous waves are derived by using these reflection coefficients. Further, a numerical example is considered to illustrate the influences of viscous cross-coupling, porosity,saturation of gas, pore-characteristics and wave frequency on the energy flux characteristics of seismic waves respectively. Specifically, the Lo-Yeh-Lee theory (LYLT) [28] considering viscous cross-coupling between two immiscible fluids in an isotropic porous solid is compared with Tuncay-Corapcioglu theory (TCT) [13], and Lo-Sposito-Majer theory (LSMT) [19] of porous solid containing two immiscible fluids. In mathematical framework, the conservation of incident energy is confirmed by considering an interaction energy between two dissimilar waves. It validates that the numerical calculations are analytically correct. Finally, some conclusions are addressed which may be drawn from the discussions of the numerical results.

2. Basic Equations

The mathematical model proposed by Lo et al. [28] has been considered as reference work, wherein equations of motion for deformable porous media containing two immiscible fluids (say, a gas and a water) incorporating the viscous cross-coupling due to relative velocity between two adjacent fluids are derived. The equations of motion, in the absence of body force, are given by

$$\begin{aligned}
\langle\tau_s\rangle_{ij,j} &= \rho_s\alpha_s\ddot{u}_i + A_{11}(\ddot{v}_i - \ddot{u}_i) + A_{12}(\ddot{w}_i - \ddot{u}_i) + A_{21}(\ddot{v}_i - \ddot{u}_i) + A_{22}(\ddot{w}_i - \ddot{u}_i) \\
&+ R_{11}(\dot{v}_i - \dot{u}_i) + R_{12}(\dot{w}_i - \dot{u}_i) + R_{21}(\dot{v}_i - \dot{u}_i) + R_{22}(\dot{w}_i - \dot{u}_i), \\
\langle\tau_1\rangle_{ij,j} &= \rho_1\alpha_1\ddot{v}_i - A_{11}(\ddot{v}_i - \ddot{u}_i) - A_{12}(\ddot{w}_i - \ddot{u}_i) - R_{11}(\dot{v}_i - \dot{u}_i) - R_{12}(\dot{w}_i - \dot{u}_i), \\
\langle\tau_2\rangle_{ij,j} &= \rho_2\alpha_2\ddot{w}_i - A_{21}(\ddot{v}_i - \ddot{u}_i) - A_{22}(\ddot{w}_i - \ddot{u}_i) - R_{21}(\dot{v}_i - \dot{u}_i) - R_{22}(\dot{w}_i - \dot{u}_i),
\end{aligned} \tag{1}$$

where u_i, v_i and w_i represent the solid, gas and water particles displacement components respectively. The indices s, 1 and 2 represent the three phases of composite medium such as solid, gas and water, respectively. Else, the variable indices in the tensors can take the values 1, 2, 3. The partial time derivative is represented by a dot over variable. The τ's are used to define stresses, ρ's are material densities and α's are volume fractions of the different phases. Coefficients A_{11} and A_{22} represent the inertial coupling of two fluid phases with solid. A_{12} (= A_{21}) identifies inertial coupling between two fluids. Coefficients R_{11} and R_{22} define the viscous coupling of two fluid phases with solid particles whereas R_{12} and R_{21} represents the viscous cross coupling between two fluids.

The stress-strain relations for the composite medium are given by

$$\begin{aligned}
\langle\tau_s\rangle_{ij} &= ((a_{11} - \frac{2}{3}G)u_{k,k} + a_{12}v_{k,k} + a_{13}w_{k,k})\delta_{ij} + G(u_{i,j} + u_{j,i}), \\
\langle\tau_1\rangle_{ij} &= (a_{12}u_{k,k} + a_{22}v_{k,k} + a_{23}w_{k,k})\delta_{ij}, \\
\langle\tau_2\rangle_{ij} &= (a_{13}u_{k,k} + a_{23}v_{k,k} + a_{33}w_{k,k})\delta_{ij},
\end{aligned} \tag{2}$$

where δ_{ij} is Kronecker symbol. G is the shear modulus of the porous frame and the elastic coefficients a_{ij} (= a_{ji}) of the porous aggregate are given in the Appendix.

Equations of motion, in terms of the displacement components are written as follows.

$$\begin{aligned}
&(a_{11} + \frac{1}{3}G)u_{j,ij} + a_{12}v_{j,ij} + a_{13}w_{j,ij} + Gu_{i,jj} = (\rho_s\alpha_s - A_{11} - A_{12} - A_{21} - A_{22})\ddot{u}_i \\
&+(A_{11} + A_{12})\ddot{v}_i + (A_{12} + A_{22})\ddot{w}_i - (R_{11} + R_{12} + R_{21} + R_{22})\dot{u}_i + (R_{11} + R_{21})\dot{v}_i + (R_{22} + R_{12})\dot{w}_i \\
&a_{12}u_{j,ij} + a_{22}v_{j,ij} + a_{23}w_{j,ij} = (A_{11} + A_{12})\ddot{u}_i + (\rho_1\alpha_1 - A_{11})\ddot{v}_i - A_{12}\ddot{w}_i \\
&+(R_{11} + R_{12})\dot{u}_i - R_{11}\dot{v}_i - R_{12}\dot{w}_i, \\
&a_{13}u_{j,ij} + a_{23}v_{j,ij} + a_{33}w_{j,ij} = (A_{21} + A_{22})\ddot{u}_i - A_{21}\ddot{v}_i + (\rho_2\alpha_2 - A_{22})\ddot{w}_i \\
&+(R_{21} + R_{22})\dot{u}_i - R_{21}\dot{v}_i - R_{22}\dot{w}_i.
\end{aligned} \tag{3}$$

3. Harmonic Plane Waves

The displacement components to study the propagation of plane harmonic wave in the medium are given by

$$(u_i, v_i, w_i) = (A_i, B_i, C_i)\exp\{i\omega(s_j x_j - t)\}, \quad (i = 1, 2, 3), \tag{4}$$

where the vectors (A_1, A_2, A_3), (B_1, B_2, B_3) and (C_1, C_2, C_3) are defined as the polarizations of the solid, gas and water particles in the composite medium respectively. The slowness vector $(s_1, s_2, s_3) = n/V$ represents the propagation/attenuation of a wave through a unit vector $n = (n_1, n_2, n_3)$ and the velocity V. By substituting (4) in (3), we get nine homogeneous equations, given by

$$[(a_{11} + \frac{1}{3}G)n_i n_j + (G - \rho_{ss}V^2)\delta_{ij}]A_j + [a_{12}n_i n_j - \rho_{s1}V^2\delta_{ij}]B_j + [a_{13}n_i n_j - \rho_{s2}V^2\delta_{ij}]C_j = 0, \quad (5)$$

$$[a_{12}n_i n_j - \rho_{1s}V^2\delta_{ij}]A_j + [a_{22}n_i n_j - \rho_{11}V^2\delta_{ij}]B_j + [a_{23}n_i n_j - \rho_{12}V^2\delta_{ij}]C_j = 0, \quad (6)$$

$$[a_{13}n_i n_j - \rho_{2s}V^2\delta_{ij}]A_j + [a_{23}n_i n_j - \rho_{21}V^2\delta_{ij}]B_j + [a_{33}n_i n_j - \rho_{22}V^2\delta_{ij}]C_j = 0, \quad (7)$$

where

$\rho_{ss} = \rho_s\alpha_s - A_{11} - A_{12} - A_{21} - A_{22} - \frac{\iota}{\omega}(R_{11} + R_{12} + R_{21} + R_{22})$,
$\rho_{s1} = A_{11} + A_{12} + \frac{\iota}{\omega}(R_{11} + R_{21})$,
$\rho_{s2} = A_{12} + A_{22} + \frac{\iota}{\omega}(R_{12} + R_{22})$,
$\rho_{1s} = A_{11} + A_{12} + \frac{\iota}{\omega}(R_{11} + R_{12})$,
$\rho_{11} = \rho_1\alpha_1 - A_{11} - \frac{\iota}{\omega}R_{11}$,
$\rho_{12} = -A_{12} - \frac{\iota}{\omega}R_{12}$,
$\rho_{2s} = A_{21} + A_{22} + \frac{\iota}{\omega}(R_{21} + R_{22})$,
$\rho_{21} = -A_{21} - \frac{\iota}{\omega}R_{21}$,
$\rho_{22} = \rho_2\alpha_2 - A_{22} - \frac{\iota}{\omega}R_{22}$.

The equations (6) and (7) are solved into two relations, given by

$$B_i = \Gamma_{ij}A_j, \quad \Gamma = \frac{b_0}{a_0}(\mathbf{I} - \mathbf{n}^T\mathbf{n}) + \frac{b_0V^4 + b_1V^2 + b_2}{a_0V^4 + a_1V^2 + a_2}\mathbf{n}^T\mathbf{n}, \quad (8)$$

$$C_i = \Delta_{ij}A_j, \quad \Delta = \frac{c_0}{a_0}(\mathbf{I} - \mathbf{n}^T\mathbf{n}) + \frac{c_0V^4 + c_1V^2 + c_2}{a_0V^4 + a_1V^2 + a_2}\mathbf{n}^T\mathbf{n}, \quad (9)$$

where, $\mathbf{I}$ is the identity matrix and $\mathbf{n}^T$ identify the transpose of the row-matrix $\mathbf{n} = (n_1, n_2, n_3)$. The above relations interrelate the polarisations (displacements) of solid particles with gas and water particles in the porous aggregate. The polarisation vector $\mathbf{A}$ defines the polarisation of solid particles in the aggregate. Polarisations of the gas and water particles are calculated from the relations (8) and (9), respectively.

where, $a_0 = \rho_{11}\rho_{22} - \rho_{12}\rho_{21}$, $a_1 = a_{23}\rho_{12} + a_{23}\rho_{21} - a_{22}\rho_{22} - a_{33}\rho_{11}$, $a_2 = a_{22}a_{33} - a_{23}^2$,
$b_0 = \rho_{12}\rho_{2s} - \rho_{1s}\rho_{22}$, $b_1 = a_{12}\rho_{22} + a_{33}\rho_{1s} - a_{13}\rho_{12} - a_{23}\rho_{2s}$, $b_2 = a_{13}a_{23} - a_{12}a_{33}$,
$c_0 = \rho_{1s}\rho_{21} - \rho_{2s}\rho_{11}$, $c_1 = a_{13}\rho_{11} + a_{22}\rho_{2s} - a_{12}\rho_{21} - a_{23}\rho_{1s}$, $c_2 = a_{12}a_{23} - a_{13}a_{22}$.

Substituting (8) and (9) in (5), we get the following relations

$$D_{ij}A_j = 0, \qquad D = a_3(\mathbf{I} - \mathbf{n}^T\mathbf{n}) + b_3\mathbf{n}^T\mathbf{n}, \quad (10)$$

$a_3 = G - (\rho_{ss} + \frac{b_0}{a_0}\rho_{s1} + \frac{c_0}{a_0}\rho_{s2})V^2$,
$b_3 = a_{11} + \frac{4}{3}G - \rho_{ss}V^2 + (a_{12} - \rho_{s1}V^2)\left(\frac{b_0V^4 + b_1V^2 + b_2}{a_0V^4 + a_1V^2 + a_2}\right) + (a_{13} - \rho_{s2}V^2)\left(\frac{c_0V^4 + c_1V^2 + c_2}{a_0V^4 + a_1V^2 + a_2}\right)$.

The system of equation (10) represent the Christoffel equations. Non-trivial solution of this system is ensured by a cubic equation (in V^2)

$$d_3V^6 + d_2V^4 + d_1V^2 + d_0 = 0, \quad (11)$$

where,

$$\begin{pmatrix} d_3 \\ d_2 \\ d_1 \\ d_0 \end{pmatrix} = \begin{bmatrix} a_0 & b_0 & c_0 \\ a_1 & b_1 & c_1 \\ a_2 & b_2 & c_2 \\ 0 & 0 & 0 \end{bmatrix} \begin{pmatrix} \rho_{ss} \\ \rho_{s1} \\ \rho_{s2} \end{pmatrix} - \begin{bmatrix} 0 & 0 & 0 \\ a_0 & b_0 & c_0 \\ a_1 & b_1 & c_1 \\ a_2 & b_2 & c_2 \end{bmatrix} \begin{pmatrix} a_{11} + \frac{4}{3}G \\ a_{12} \\ a_{13} \end{pmatrix},$$

and a linear equation (in V^2), given by

$$G - (\rho_{ss} + \frac{b_0}{a_0}\rho_{s1} + \frac{c_0}{a_0}\rho_{s2})V^2 = 0. \tag{12}$$

The three roots of the cubic equation (11) explains the existence of three longitudinal waves (i.e., polarization vector is parallel to propagation vector) propagating with velocities ($V_j,\ j = 1, 2, 3$). For convenience, the three longitudinal waves identified with velocities $V_1,\ V_2$ and V_3 are termed as P_1, P_2 and P_3 wave, respectively.

In an analogs manner, the single root of equation (12), explains the existence of lone transverse wave (i.e., polarization vector is normal to propagation vector) propagating with velocity V_4, given by the relation $V_4^2 = G/(\rho_{ss} + \frac{b_0}{a_0}\rho_{s1} + \frac{c_0}{a_0}\rho_{s2})$. This lone transverse wave is identified as SV wave.

4. Reflection at Plane Boundary

In this study our goal is to analyze the effects of viscous cross-coupling, porosity, saturation of gas, pore-characteristics and wave frequency on the energy shares of various reflected inhomogeneous waves at the stress free surface of partially porous solid.

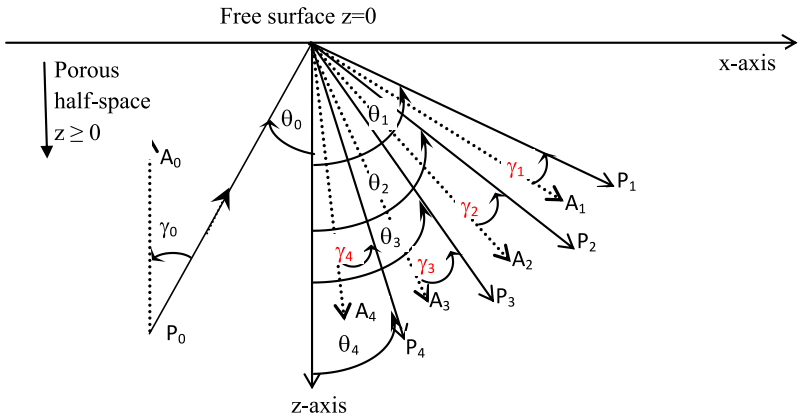

Figure 1. Geometrical Figure

4.1. Definition of the Problem

Consider a rectangular coordinate system (x, y, z), in which half-space $z > 0$ is occupied by a saturated porous solid with its depth increasing along the z-direction as shown in geometrical Figure 1. The plane $z = 0$ is considered as stress free surface of this medium. Following Borcherdt [29], in terms of angle of propagation (θ_0), angle of attenuation (γ_0), propagation vector (**P**) and attenuation vector

(**A**), the horizontal slowness is defined as

$$s = |\mathbf{P}| \sin\theta_0 - \iota|\mathbf{A}| \sin(\theta_0 - \gamma_0), \tag{13}$$

where, for incident wave of velocity V_0, we have

$$|\mathbf{P}|^2 = \frac{1}{2}[Re(\frac{\omega^2}{V_0^2}) + \sqrt{(Re(\frac{\omega^2}{V_0^2}))^2 + (Im(\frac{\omega^2}{V_0^2}))^2/\cos^2\gamma_0}], \tag{14}$$

$$|\mathbf{A}|^2 = \frac{1}{2}[-Re(\frac{\omega^2}{V_0^2}) + \sqrt{(Re(\frac{\omega^2}{V_0^2}))^2 + (Im(\frac{\omega^2}{V_0^2}))^2/\cos^2\gamma_0}]. \tag{15}$$

Due to the dissipative nature of porous medium, the incident wave at the boundary $z = 0$ is specified through its propagation direction (θ_0) and attenuation direction (γ_0). The vector $(s, 0, q_0)$ specify the slowness vector of incident wave, where $q_0(= \pm\sqrt{V_0^2 - s^2})$ is the vertical slowness of incident wave. To ensure the propagation of incident wave towards the boundary (i.e., negative z-direction), we must have $\Re(q_0) < 0$. According to Snell's law the horizontal slowness (s) of both incident and reflected waves will be remains same. Then, the vector $(s, 0, q_k)$ specify the slowness vector for reflected waves, where $q_k = \pm\sqrt{V_k^2 - s^2}, (k = 1, 2, 3, 4)$. To assure the decay of reflected waves moving away from boundary (i.e., positive z-direction), we must have $\Im(q_k) > 0$. Then, the total displacement of material particles of medium is the sum of displacements associated with incident wave and three reflected waves. Hence, for two dimensional motion in xz-plane, the general displacement of material particles is expressed as

$$\begin{aligned}
u_j &= [A_j^{(0)} \exp\{\iota\omega(sx - q_0 z - t)\} + \sum_{k=1}^{4} f_k A_j^{(k)} \exp\{\iota\omega(sx + q_k z - t)\}],\\
v_j &= [B_j^{(0)} \exp\{\iota\omega(sx - q_0 z - t)\} + \sum_{k=1}^{4} f_k B_j^{(k)} \exp\{\iota\omega(sx + q_k z - t)\}],\\
w_j &= [C_j^{(0)} \exp\{\iota\omega(sx - q_0 z - t)\} + \sum_{k=1}^{4} f_k C_j^{(k)} \exp\{\iota\omega(sx + q_k z - t)\}], \quad (j = x, z),
\end{aligned} \tag{16}$$

where, f_k are the excitation factors for reflected waves relative to incident wave. The index "0" represent the incident wave. The index "k"$(= 1, 2, 3, 4)$ represent, respectively, the reflected (P_1, P_2, P_3, SV) waves. To define polarization of a longitudinal and transverse wave, the required unit vector **n** is obtained as $\mathbf{n} = (s, 0, q_k)V_k$.

4.2. Boundary Conditions

In the present geometry, boundary conditions for the particle motion are considered at the stress free plane surface $z = 0$. In this problem,we consider two kinds of boundary conditions at the plane $z = 0$, one is impermeable boundary (sealed pores) and other is permeable boundary (fully-opened pores). In case of impermeable boundary (sealed pores), no discharge of interstitial fluid is allowed at the surface with the passage of waves. While in case of permeable boundary (fully-opened pores),

the fluid pressure should be vanish at the plane $z = 0$. Hence, the suitable boundary conditions to be satisfied at the plane $z = 0$ are given by

$$\begin{aligned} &i)\ \langle \tau_s \rangle_{zz} = 0, \\ &ii)\ \langle \tau_s \rangle_{zx} = 0, \\ &iii)\ \zeta T_0 \dot{v}_z - (1-\zeta)\langle \tau_1 \rangle_{zz} = 0, \\ &iv)\ \zeta T_0 \dot{w}_z - (1-\zeta)\langle \tau_2 \rangle_{zz} = 0, \end{aligned} \tag{17}$$

where, T_0 is a scaling parameter that ensures dimensional homogeneity. The parameter $\zeta = 1$ define the impermeable boundary (sealed surface-pores) and $\zeta = 0$ define the permeable boundary (fully-opened surface-pores).

4.3. Reflection Coefficients

We obtain a system of four simultaneous non-homogeneous linear equations after solving the four boundary conditions (17) using displacements defined in equation (16). The system of four equations, are given by

$$\sum_{k=1}^{4} b_{lk} f_k = -b_{l0}, \qquad (l = 1, 2, 3, 4). \tag{18}$$

For $(k = 1, 2, 3, 4)$, we have
$b_{1k} = (a_{11} - 2G/3)[sA_x^{(k)} + q_k A_z^{(k)}] + a_{12}[sB_x^{(k)} + q_k B_z^{(k)}] + a_{13}[sC_x^{(k)} + q_k C_z^{(k)}] + 2Gq_k A_z^{(k)}$,
$b_{2k} = G[q_k A_x^{(k)} + sA_z^{(k)}]$, $\quad b_{3k} = \zeta T_0 B_z^{(k)} - (1-\zeta) Y_k$, $\quad b_{4k} = \zeta T_0 C_z^{(k)} - (1-\zeta) Z_k$,
where, $Y_k = a_{12}[sA_x^{(k)} + q_k A_z^{(k)}] + a_{22}[sB_x^{(k)} + q_k B_z^{(k)}] + a_{23}[sC_x^{(k)} + q_k C_z^{k}]$
and $Z_k = a_{13}[sA_x^{(k)} + q_k A_z^{(k)}] + a_{23}[sB_x^{(k)} + q_k B_z^{(k)}] + a_{33}[sC_x^{k} + q_k C_z^{(k)}]$.

System (18) is solved for four unknowns $f_k (k = 1, 2, 3, 4)$ by using Gauss elimination method. These unknown may be treated as reflection coefficients.

4.4. Energy Partition

In this article, our goal is to study the partition of incident wave energy into distinct reflected waves. The energy communicated per unit area at the plane $z = 0$ is the scalar product of surface traction and particle velocity (Achenbach[30]). Due to dissipative nature of porous medium, the concept of interaction energy (Borcherdt [29]; Krebes [31]) or the interference energy (Ainslie and Burns [32]) between two dissimilar waves is also involved. Therefore, total energy flux is the sum of energy flux carried out by reflected waves and interaction energy between two dissimilar waves. In the present geometry, medium supports the propagation of four (one incident and three reflected) waves. Hence, to described the distribution of incident energy at the surface $z = 0$, an energy matrix is defined as

$$E_{lk} = \Re(P_{lk} f_l \bar{f}_k)/\Re(P_{55}), \qquad (l, k = 1, 2, 3, 4, 5); \tag{19}$$

where $f_5 = 1$. A bar over a complex quantity denotes conjugate. The elements P_{lk} in equation (19) are given by

$$P_{lk} = \left[(a_{11} - 2G/3)[sA_x^{(l)} + q_l A_z^{(l)}] + a_{12}[sB_x^{(l)} + q_l B_z^{(l)}] + a_{13}[sC_x^{(l)} + q_l C_z^{(l)}] + 2Gq_l A_z^{(l)}\right] \bar{A}_z^{(k)}$$

$$+ \quad G\left[sA_z^{(l)} + q_l A_x^{(l)}\right]\bar{A}_x^{(k)} + Y_l\bar{B}_z^{(k)} + Z_l\bar{C}_z^{(k)}. \tag{20}$$

The energy matrix $E_{ij},\ (i, j = 1, 2, 3, 4)$, calculates the energy shares of three reflected $(P_1,\ P_2, P_3,\ SV)$ waves in porous medium. The diagonal entries $E_{11},\ E_{22},\ E_{33}$ and E_{44} identify the energy shares of reflected $P_1,\ P_2,\ P_3$ and SV waves, respectively. The interaction energy due to the interference of each reflected wave with incident wave is given by $E_{IR} = \sum_{i=1}^{4}(E_{5i} + E_{i5})$. The interaction energy due to the interference between each pair of reflected waves is given by $E_{RR} = \sum_{i=1}^{4}(\sum_{j=1}^{4} E_{ij} - E_{ii})$. Then, conservation of energy at the stress free surface is assured through the relation $\sum_{l=1}^{5}\sum_{k=1}^{5} E_{lk} = 0$.

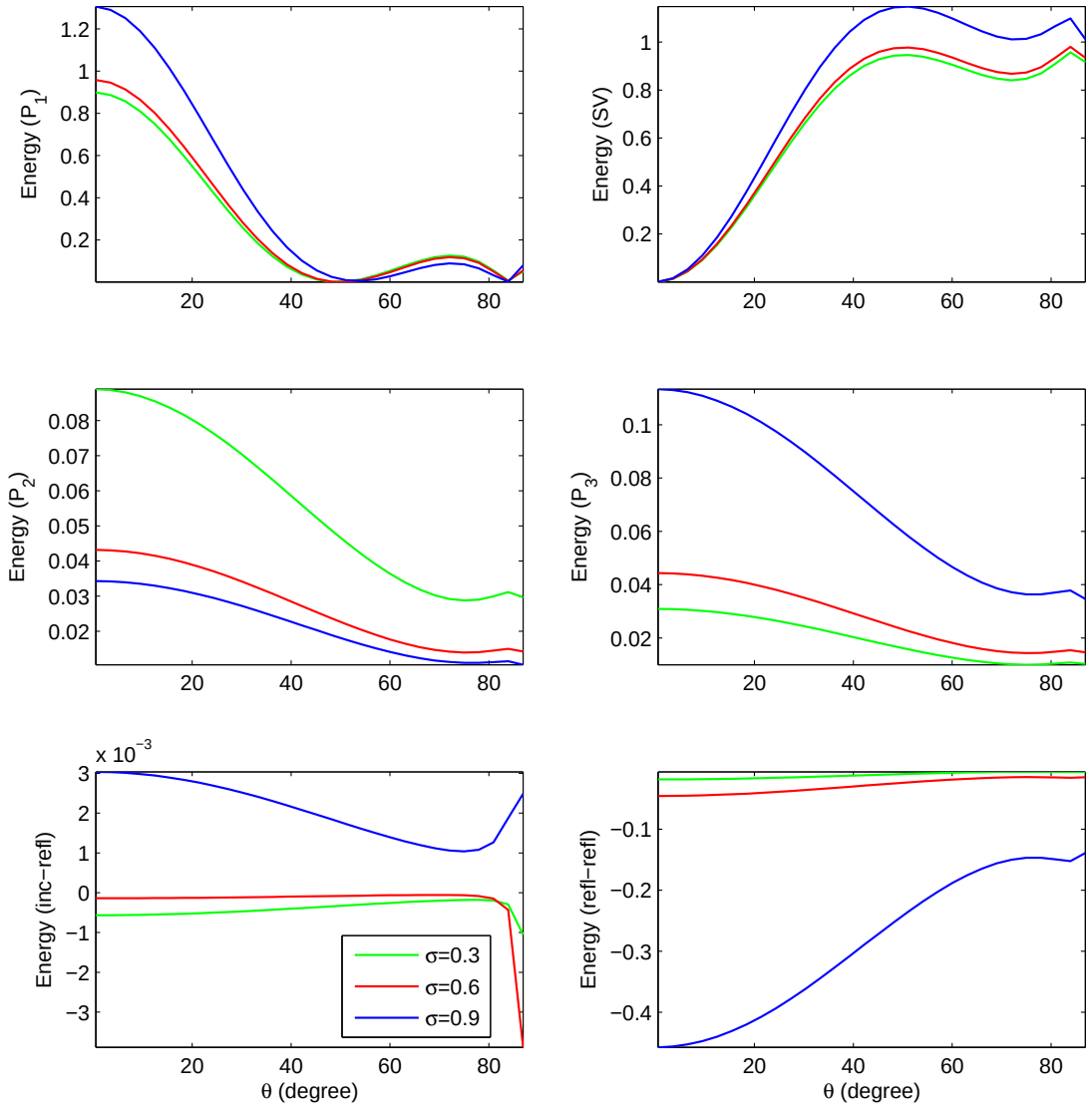

Figure 2. Variations in energy partition with incident direction (θ_0) and gas saturation (σ); $\phi = 0.45,\ \omega = 2\pi kHz,\ \gamma_0 = 45^0,\ \nu = 0.2,\ \zeta = 1$; incident P_1 wave.

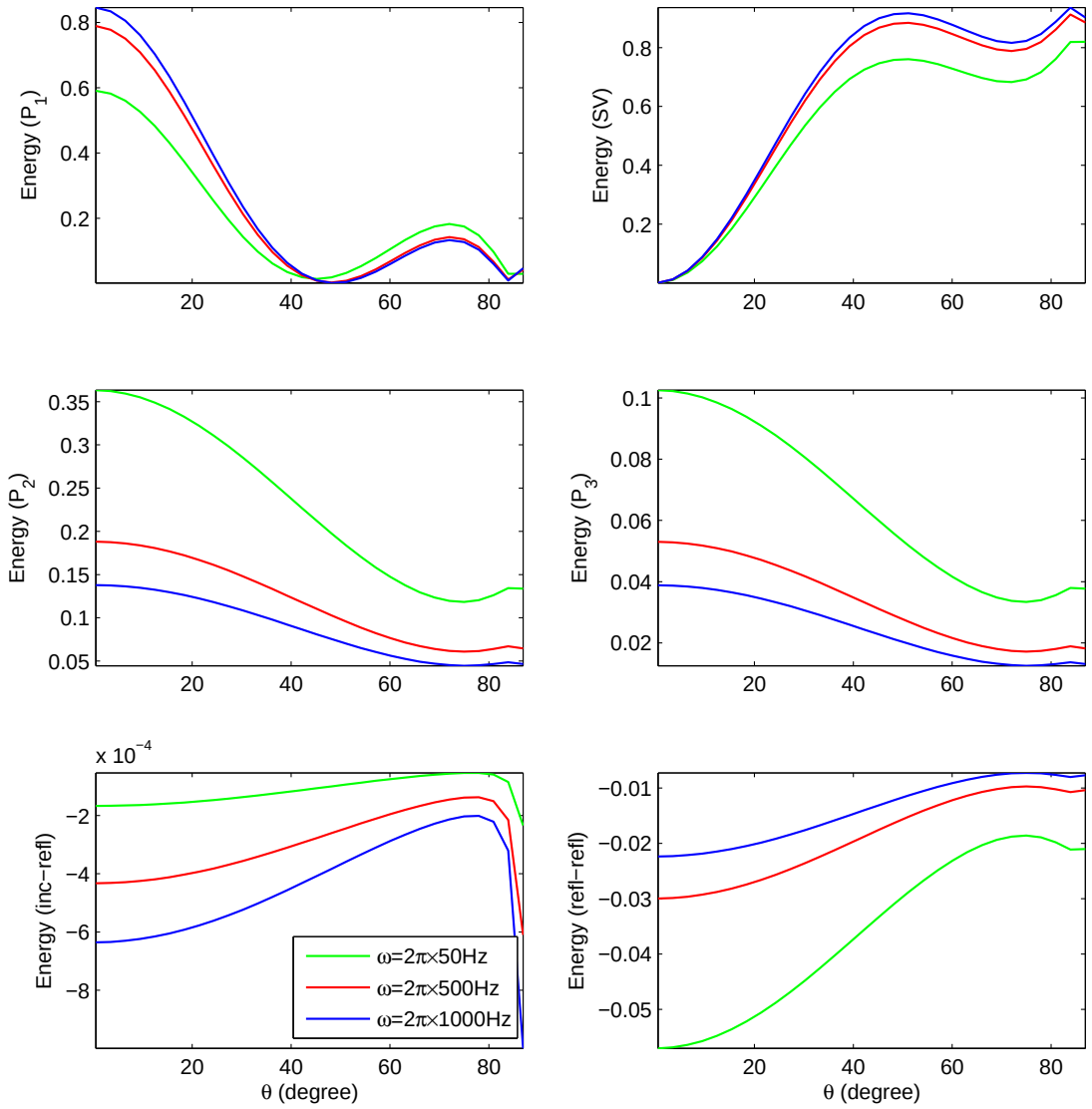

Figure 3. Variations in energy partition with incident direction (θ_0) and frequency (ω); $\phi = 0.45,\ \sigma = 0.2,\ \gamma_0 = 45^0,\ \nu = 0.1,\ \zeta = 1$; incident P_1 wave.

5. Numerical Results and Discussion

5.1. Numerical Example

The main purpose of this study is to analyze the effects of viscous cross-coupling, porosity, saturation of gas, pore-characteristics and wave frequency on the energy shares of various reflected inhomogeneous waves at the stress free surface of partially porous solid. Numerical study is carried out by Matlab. Hence, a numerical example is considered. To choose the numerical values of various param-

eters, we consider a reservoir rock (sandstone) saturated with water and CO_2. The values of relevant material and fitting parameters (Garg and Nayfeh [8]; Lo et al. [19]) are given in Table 1.

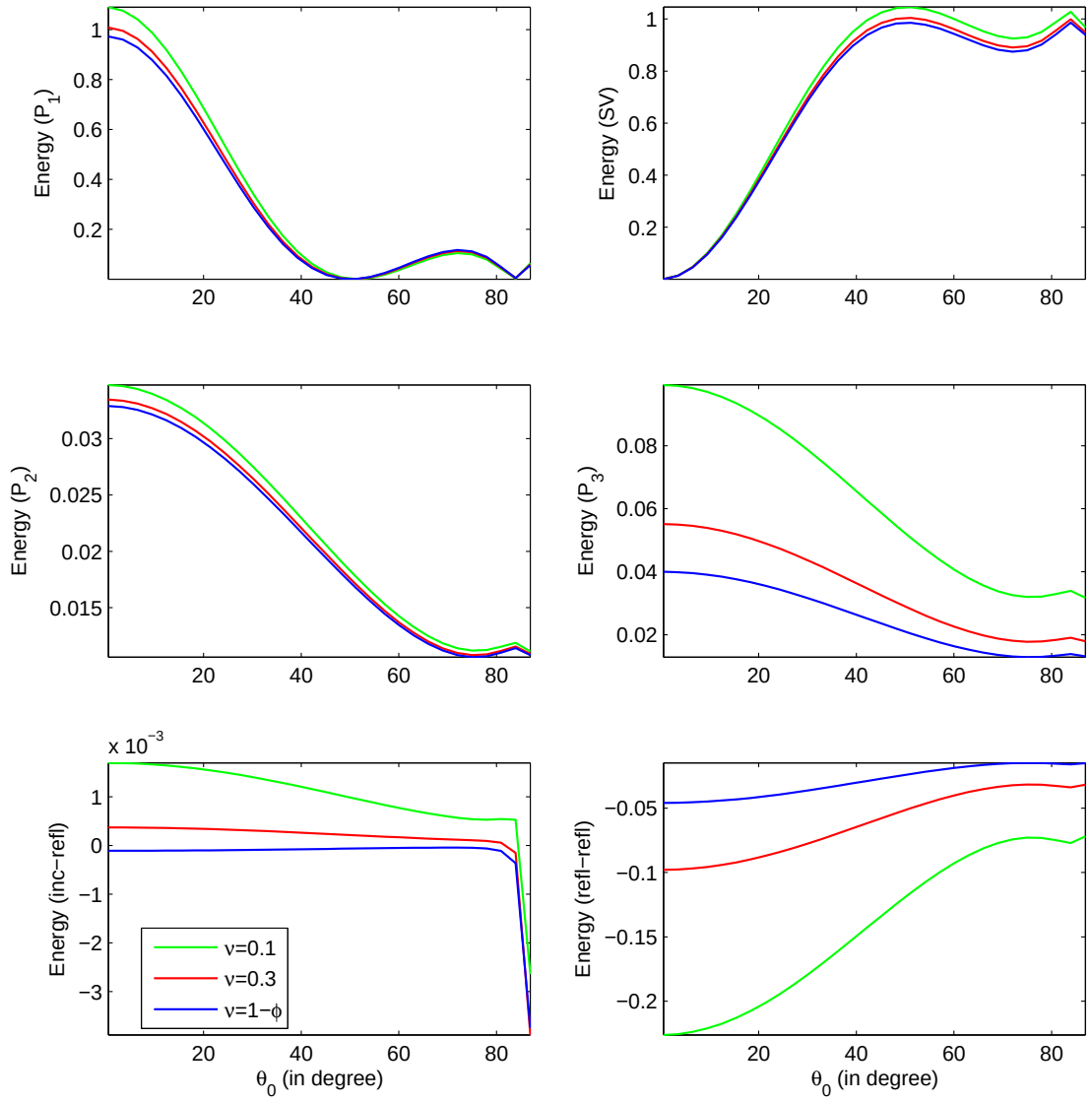

Figure 4. Variations in energy partition with incident direction (θ_0) and viscous cross-coupling parameter (ν); $\phi = 0.45,\ \omega = 2\pi \times kHz,\ \sigma = 0.8,\ \gamma_0 = 45^0,\ \zeta = 1$; incident P_1 wave.

5.2. Discussion of Numerical Results

The partitions of incident energy among various reflected waves and interaction energy between two distinct waves is defined by the energy matrix E in the section 4.4. The variations of these energy shares with incident direction ($\theta_0 \in (0,\ 90^0)$) are presented in figures 2 to 7 (for incident P_1 wave) and

in figures 8 to 13 (for incident $S\,V$ wave). The detailed discussion on figures is as follows.

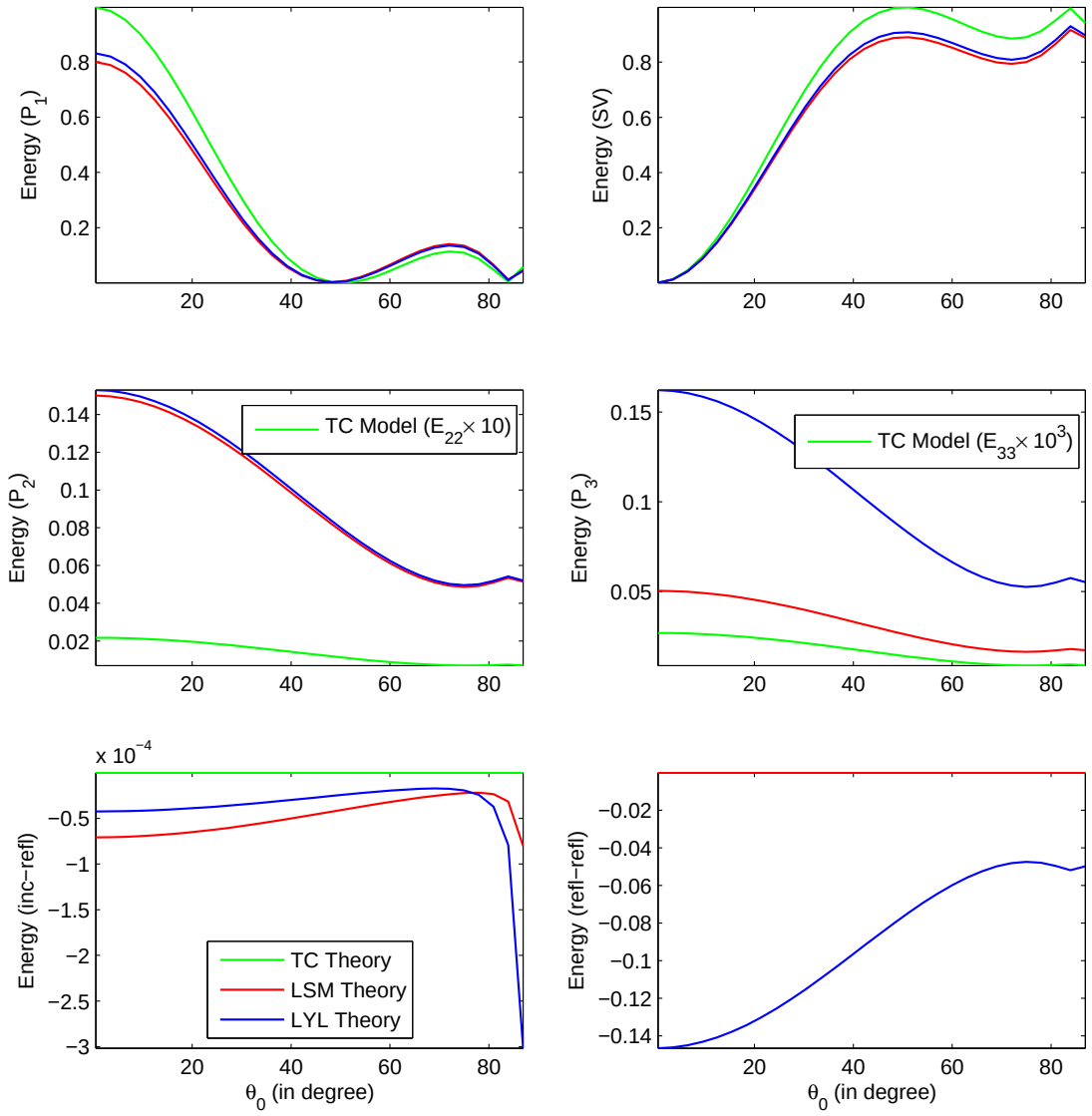

Figure 5. Variations in energy partition with incident direction (θ_0), corresponding to three different theories; $\sigma = 0.5,\ \phi = 0.45,\ \omega = 2\pi \times 100Hz,\ \gamma_0 = 45^0,\ \zeta = 1$; incident P_1 wave.

5.2.1. For the Incidence of P_1 Wave

Figure 2 presents the essence of incident direction (θ_0) and gas saturation (σ) on the various energy shares and interaction energies. A significant effect of gas saturation is clearly seen on all the reflected waves and interaction energy between two dissimilar waves. For the incidence below 55^0, P_1 wave strengthens with the increase of gas shares in pores. However, beyond 55^0 it weakens slightly with

this change. The SV wave strengthens with the increase of gas share in pores, particularly beyond 25^0. Further, it is clear that $P_2(P_3)$ wave weakens (strengthens) with the increase of gas share in pores. Near normal (grazing) incidence domination shift in favour of $P_1(SV)$ wave. In the mathematical framework, energy conservation at the boundary is confirmed by considering the interference energy between two dissimilar waves.

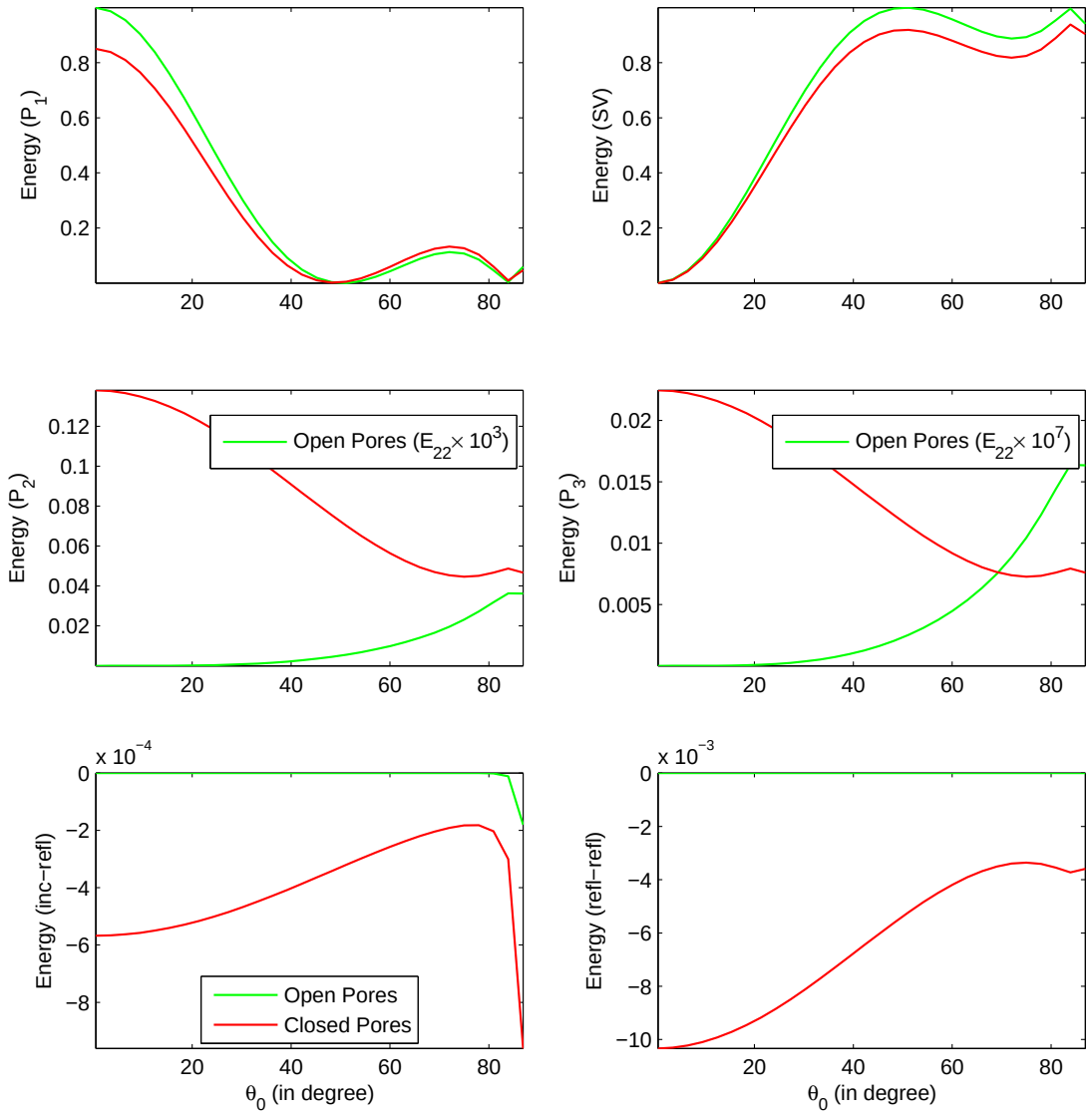

Figure 6. Variations in energy partition with incident direction (θ_0), corresponding to open and sealed surface-pores; $\phi = 0.45$, $\omega = 2\pi \times kHz$, $\sigma = 0.2$, $\gamma_0 = 45^0$, $\nu = 0.3$; incident P_1 wave.

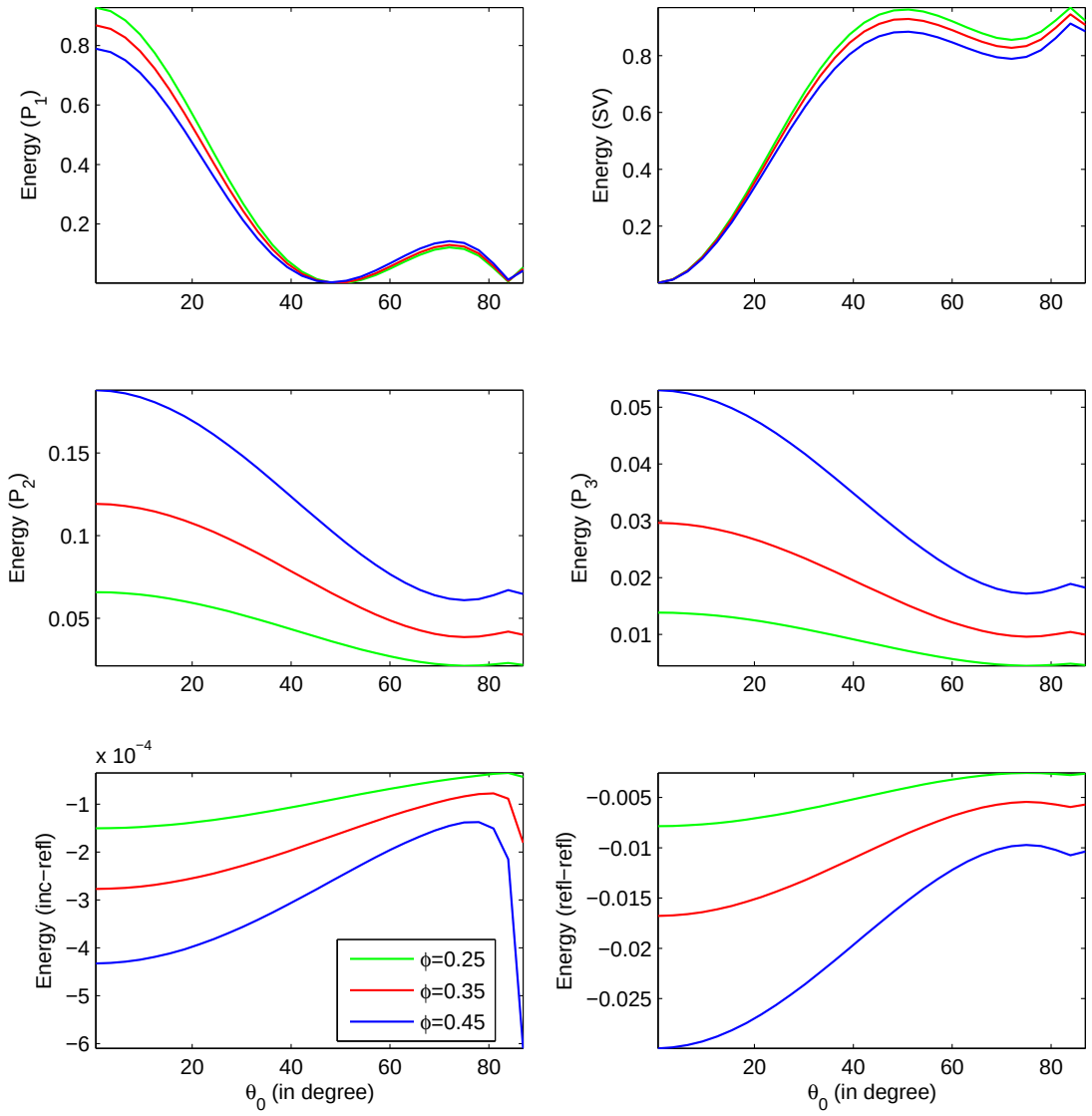

Figure 7. Variations in energy partition with incident direction (θ_0) and porosity (ϕ); $\omega = 2\pi \times 500Hz,\ \sigma = 0.2,\ \gamma_0 = 45^0,\ \nu = 0.1,\ \zeta = 1$; incident P_1 wave.

Figure 3 displays the essence of frequency on the various energy shares. The P_1 wave strengthens with the increase of frequency and beyond incidence 50^0, it weakens with the increase of frequency. For incidence beyond 20^0, SV wave strengthens with the increase of frequency. Further, it is noted that qualitative behaviour of P_2 and P_3 waves are alike. All the waves are dispersive in nature.

Figure 4 shows the effect of viscous cross-coupling parameter (ν) on the various energy shares with the incident direction θ_0. The negligible influence of viscous cross-coupling is visible on the P_1, P_2 and SV waves. Whereas, a significant effect of viscous cross-coupling is noticed on the propagation of P_3 wave and interaction energies. All the waves are weakens with the increase of viscous cross-coupling.

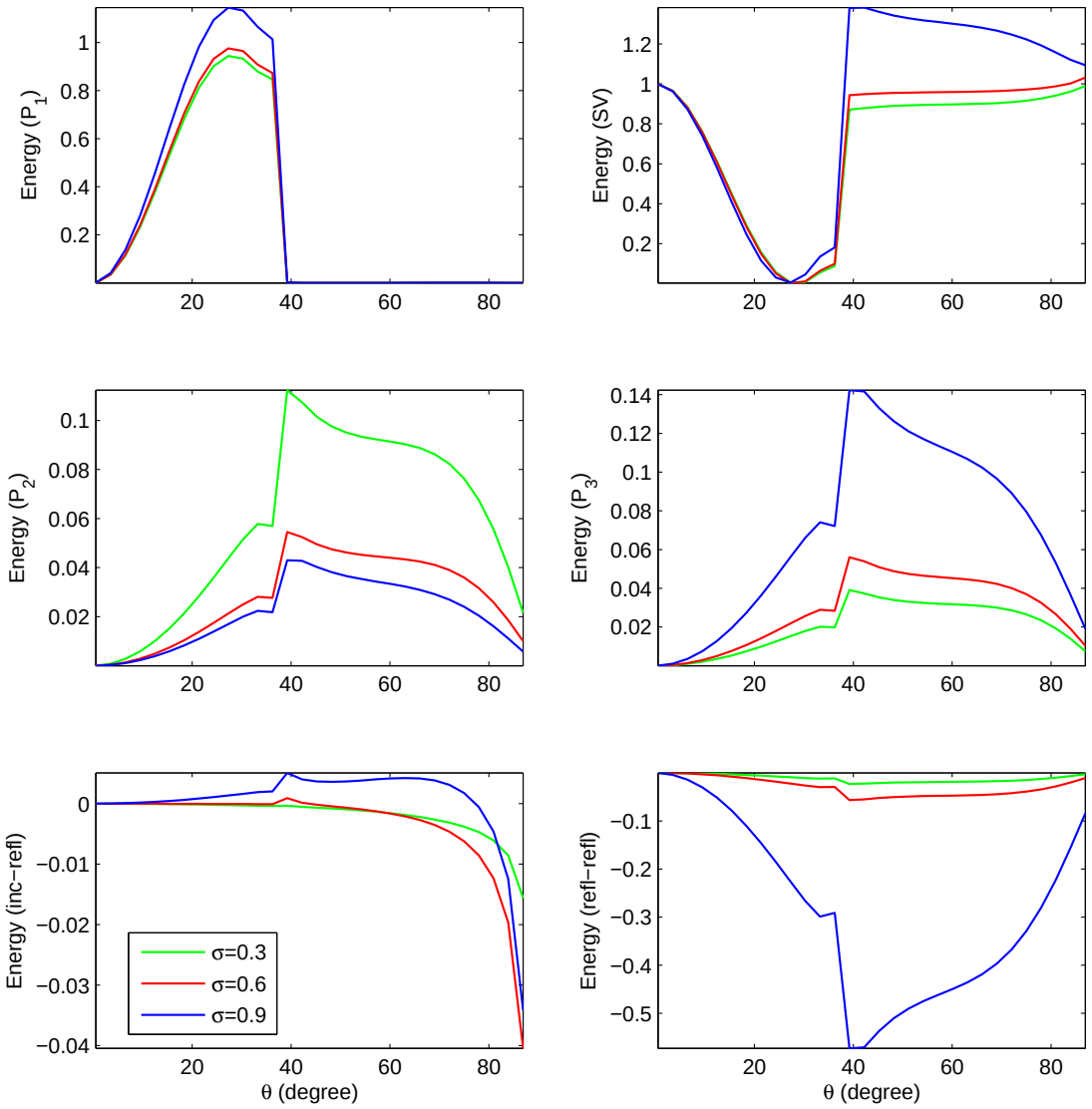

Figure 8. The same as the Figure 2 but for incident SV wave.

Figure 5 displays the variations of various energy shares with incident direction (θ_0), corresponding to three different theories. Mathematical theory presented by Lo et al. [28] (LYLT) incorporated the viscous cross-coupling between two immiscible pore fluids. It is observed that after neglecting the viscous cross-coupling terms from equations of motion, the LYLT reduces to LSMT. Further, in the absence of both inertial coupling and viscous cross-coupling terms, it reduces to TCT. It is clear that the qualitative behaviour of all energy shares are alike in all the three different theories.

In case of P_3 wave, a significant quantitative difference between these theories appear. Further, the energy shares of P_1 and SV waves are maximum for TCT and minimum for LYLT. While, the energy shares of reflected P_2 and P_3 waves are maximum for LYLT and minimum for TCT. A weaker

quantitative difference in all energy shares is observed corresponding to LYLT and LSMT except the energy share of P_3 wave.

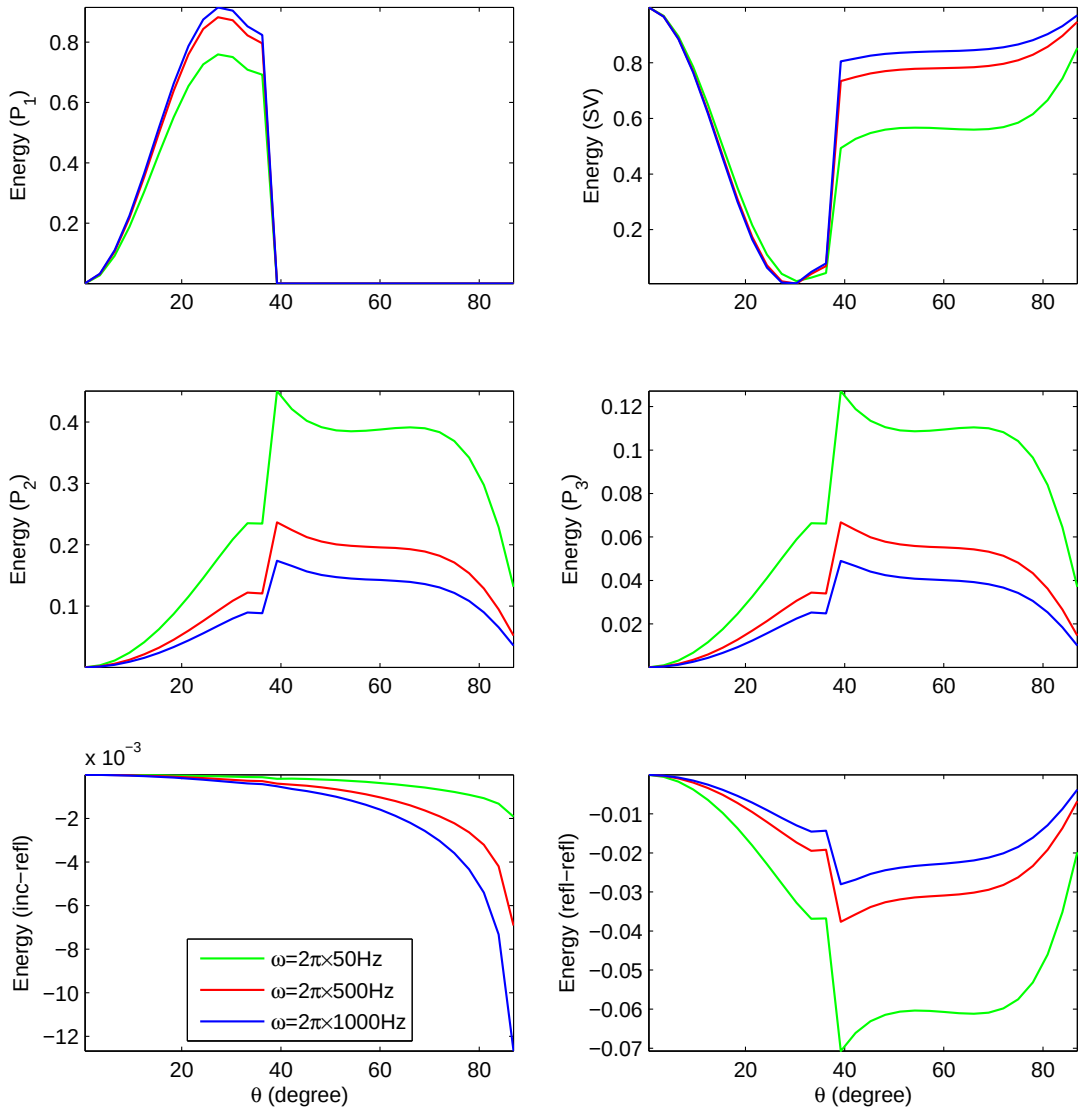

Figure 9. The same as the Figure 3 but for incident SV wave.

The variations in energy partition with incident direction (θ_0), corresponding to open and sealed surface-pores is depicted in Figure 6. A permeable boundary surface reflect a stronger P_1 wave, below the incidence 50^0. The reflected SV wave at permeable boundary (fully-opened surface-pores) is almost dominated on impermeable boundary (sealed surface-pores), for $\theta_0 \in (0,\ 90^0)$. Further, a large quantitative difference is noticed in the reflected P_2 and P_3 waves at permeable and impermeable boundary. At impermeable (permeable) boundary, the P_2 and P_3 waves are significant (insignificant).

The effect of porosity on the various energy partition is shown in Figure 7. The effect of porosity on P_1 wave is quite significant below the incidence 55^0. Whereas, for the incidence beyond 30^0, a little bit essence of porosity is observed on the SV wave. Further, reflected P_2 and P_3 waves becomes stronger with the increase in porosity.

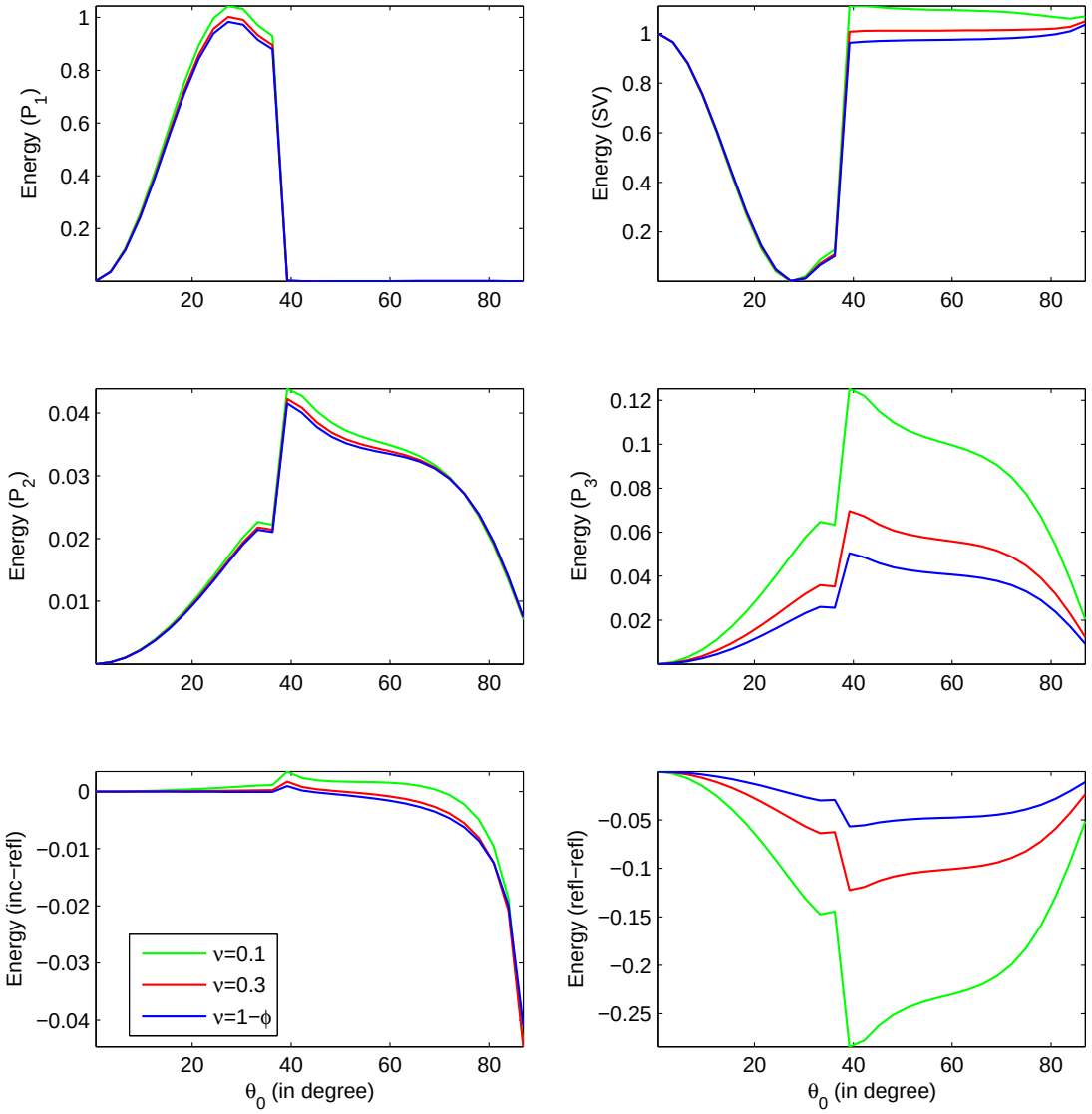

Figure 10. The same as the Figure 4 but for incident SV wave.

5.2.2. For the Incidence of SV Wave

Figure 8 displays the variations of energy shares with incident direction (θ_0) and gas saturation (σ). Alike the incident P_1 wave in Figure 2, a significant essence of gas saturation is clearly visible on all the energy shares. The critical angles are found for P_1 and SV waves around 40^0 and 28^0, respectively.

Variational pattern of P_1 wave shows a reverse behaviour to that of the SV wave. For the incidence below 40^0, P_1 wave strengthens with the increase of gas saturation. Whereas, for the incidence beyond 40^0, SV wave strengthens with the increase of gas shares in pores. Moreover, $P_2(P_3)$ wave weakens (strengthens) with the increase of gas shares in pores. For near normal incidence, it is observed only SV wave survive quantitatively.

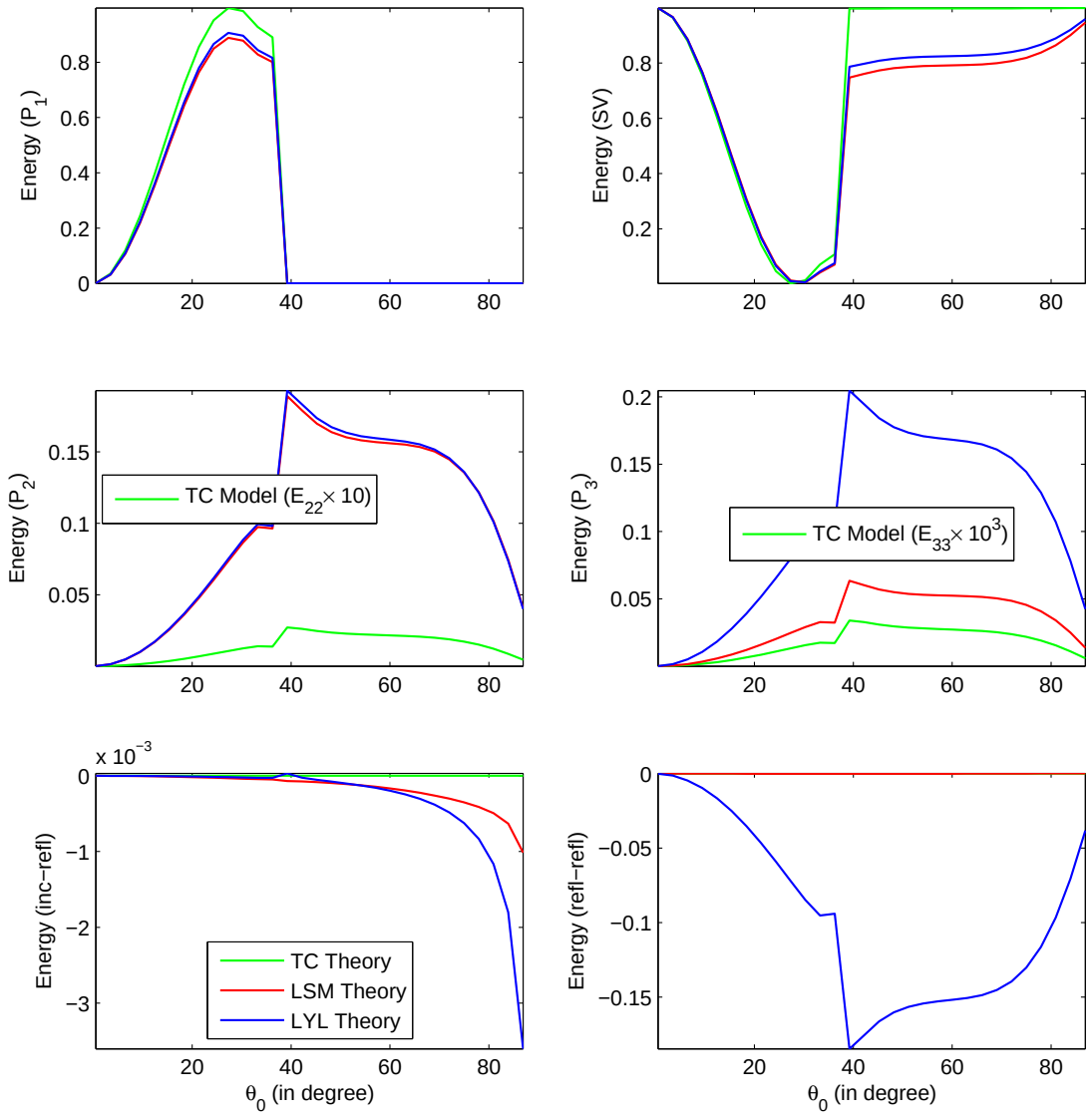

Figure 11. The same as the Fig. 5 but for incident SV wave.

Figure 9 displays the effect of wave frequency (ω) on the various energy shares. With the increase of wave frequency, P_1 and SV waves becomes quite stronger but P_2 and P_3 waves becomes weaker with this change. Further, variational pattern of P_2 and P_3 waves are almost alike.

Figure 10 shows the essence of viscous cross-coupling parameter (ν) on the various energy shares. Almost all the energy shares decreases with the increase of viscous cross-coupling. The effect of viscous cross-coupling on P_1, P_2 and SV waves is little bit significant.

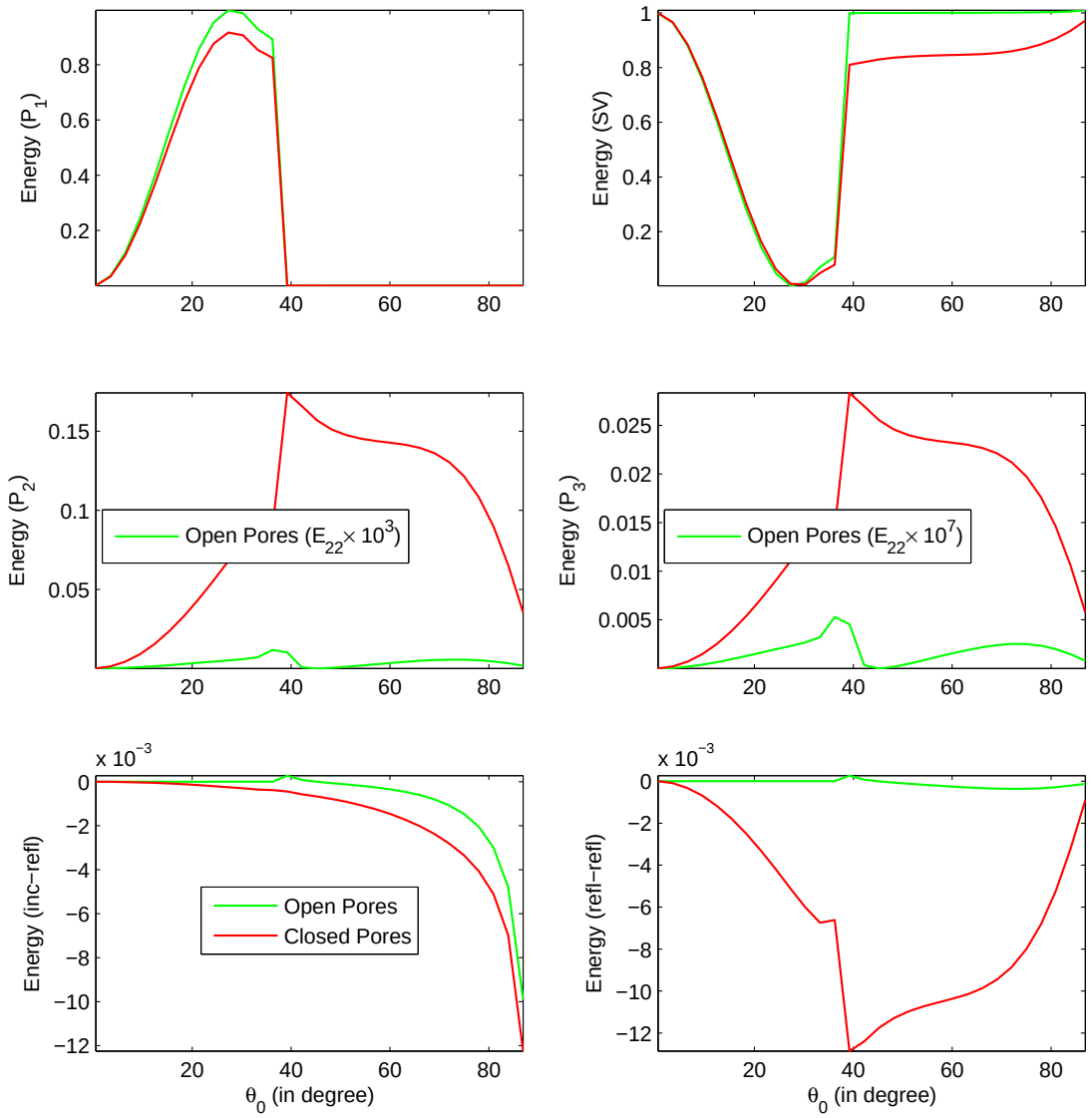

Figure 12. The same as the Fig. 6 but for incident SV wave.

The variations in energy partition with incident direction (θ_0), corresponding to three different theories are shown in Figure 11. In case of P_3 wave, a significant difference is observed between these theories. Whereas, in case of P_1, P_2 and SV waves, a insignificant difference is observed between LYLT and LSMT.

The variations in energy partition with incident direction (θ_0), corresponding to open and sealed

surface-pores is depicted in Figure 12. The observation found corresponding to these surface-pores characteristics are nearly same as the case of incident P_1 wave in Figure 6.

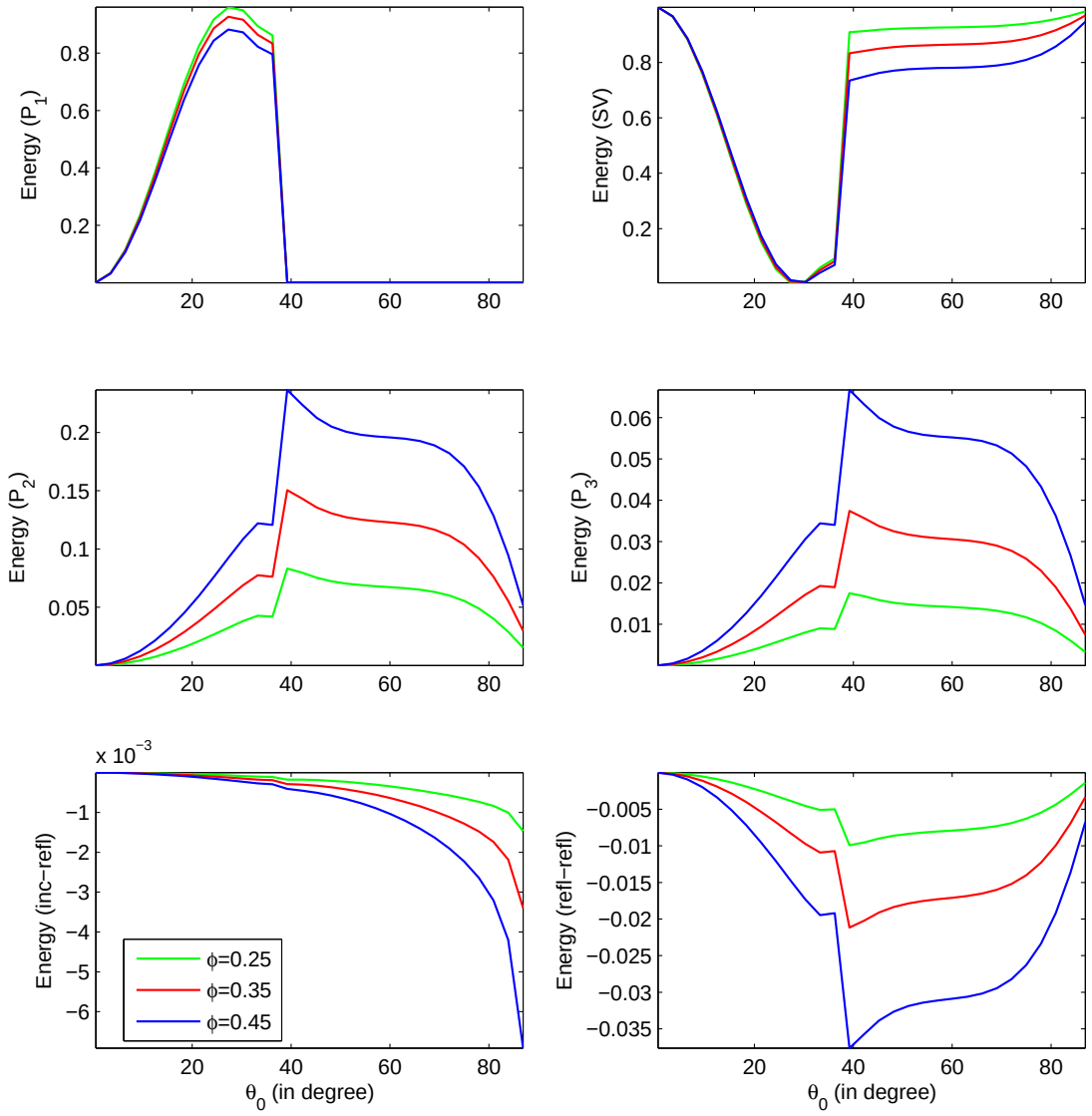

Figure 13. The same as the Figure 7 but for incident SV wave.

The effect of porosity on the various energy shares with incident direction θ_0 is shown in Fig. 13. It is clearly visible that for incidence below 40^0, P_1 wave strengthens with the increase of porosity and beyond 40^0, SV wave strengthens with the increase of porosity. Further, P_1 and P_2 waves also strengthens with the increase of porosity.

6. Conclusions

In this article, reflection of inhomogeneous waves at the stress-free plane surface of partially saturated porous solid is investigated. Porous medium is considered dissipative due to the involvement of viscosity in pores fluid. Four waves (three longitudinal and one shear) are found to be reflected, as a result of incident wave. All the reflected waves are inhomogeneous in nature (i.e., different direction of propagation and attenuation). Appropriate boundary conditions are used for opened surface-pores (permeable boundary) and fully closed surface-pores (impermeable boundary). For both incident P_1 and SV waves, energy flux characteristics of seismic waves are studied analytically and numerically for a particular model. The closed-form analytical expressions for the reflection coefficients of various reflected waves are computed analytically at the stress-free plane surface. Further, these reflection coefficients are used to calculate the energy shares of various reflected waves. Conservation of the incident energy at the plane interface is confirmed by considering the interaction energy between two dissimilar waves. Finally, for particular model, effect of hydrological properties (like, viscous cross-coupling, porosity, saturation of gas, pore-characteristics) and wave frequency has been studied on energy flux characteristics of seismic waves. The energy flux characteristics correspond to the TCT, LSMT and LYLT are also presented in this study. Finally, some conclusions are addressed which may be drawn from the discussions of the numerical results.

- At the normal incidence of SV wave, only SV wave is survive quantitatively among all the reflected waves. While at the normal incidence of P_1 wave, only SV wave is not survive quantitatively.
- The P_2 wave weakens but P_3 wave strengthens, with the increase of gas saturation.
- For both incident P_1 and SV waves, P_2 and P_3 waves are found to be strengthens (weakens), with the increase of porosity (frequency).
- The P_2 and P_3 waves are strengthens (weakens) when the pores at the reflecting boundary are fully-closed (fully-opened). Whereas, P_1 and SV waves are weakens (strengthens) when the pores at the reflecting boundary are fully-closed (fully-opened).
- The basic difference between TCT, LSMT and LYLT is mainly observed in the behaviour of P_2 and P_3 waves. Due to the involvement of viscous cross-coupling between two fluids in the equations of motion, energy shares of P_2 and P_3 waves are found to be strengthen.
- The energy shares of P_3 wave is found to be greatly influenced due to the involvement of viscous cross-coupling terms in the equations of motion. Hence, this fact shows that the present study is in good agreement with the Lo et al. [28] study. This is due to the fact that Lo et al. [28] study shows that the presence of viscous cross-coupling between two fluids, significantly influenced the phase speed of P_3 wave.
- All the waves are dispersive (i.e., frequency dependent) in nature.
- In mathematical framework, the conservation of the incident energy is confirmed by considering the interaction energy between two dissimilar waves due to the dissipative nature of the considered medium. This validates that the numerical calculations are analytically correct.

Finally, for both incident P_1 or SV wave, it is found that the energy flux characteristics of seismic waves depend on several factors, such as wave frequency, gas saturation, porosity, pore-characteristics and viscous-cross coupling between two fluids. Therefore, the study of energy flux characteristics can yield to useful information about the rock properties.

Table 1. Material and fitting parameters of a reservoir rock (sandstone) saturated with water and CO_2.

Parameter	Symbol	Value
Bulk modulus of gas	K_1	$3.7MPa$
Bulk modulus of solid	K_s	$35GPa$
Bulk modulus of the porous framework	K_b	$12GPa$
Shear modulus of the porous framework	G	$9GPa$
Bulk modulus of water	K_2	$2.25GPa$
Fitting parameter	n	2.145
Fitting parameter	η	0.5
Fitting parameter	χ	$1m^{-1}$
Material density of gas	ρ_1	$103Kg/m^3$
Material density of solid	ρ_s	$2650Kg/m^3$
Material density of water	ρ_2	$990Kg/m^3$
Intrinsic permeability of porous framework	k_s	$5.3\times10^{-13}m^2$
Viscosity of gas	μ_1	$18\times10^{-6}Ns/m^2$
Viscosity of water	μ_2	$0.001Ns/m^2$

Apendix

Following Lo et al. [21], the elasticity coefficient a_{ij} in terms of directly measurable parameters are given as

$a_{11} = K_0[\alpha_0 N_1\{K_1K_2 + K_1N_2\sigma + K_2N_2(1-\sigma)\} + K_bK_0(1-\alpha_0)\{K_1(1-\sigma) + K_2\sigma + N_2\}]/N_3,$

$a_{12} = [K_0K_1(1-\alpha_0)\sigma N_1(K_2+N_2)]/N_3, \quad a_{13} = [K_0K_2(1-\alpha_0)(1-\sigma)N_1(K_1+N_2)]/N_3,$

$a_{22} = [K_1(1-\alpha_0)\sigma\{K_0^2(1-\alpha_0)(\sigma K_2 + N_2) + K_2(1-\sigma)N_1N_2\}]/N_3,$

$a_{23} = -[K_1K_2(1-\alpha_0)(1-\sigma)\sigma\{N_1N_2 - (1-\alpha_0)K_0^2\}]/N_3,$

$a_{33} = [K_2(1-\alpha_0)(1-\sigma)\{K_0^2(1-\alpha_0)(K_1(1-\sigma)+N_2) + K_1\sigma N_1N_2\}]/N_3,$

$\frac{dp_c}{d\sigma} = (\rho_2 g/(n-1)m)[\{(1-\sigma)^{-(\frac{n}{n-1})} - 1\}^{(\frac{1-n}{n})}(1-\sigma)^{-(\frac{2n-1}{n-1})}],$

$N_1 = K_0\alpha_0 - K_b, \quad N_2 = \frac{dp_c}{d\sigma}\sigma(1-\sigma),$

$N_3 = [N_1\{K_1N_2\sigma + K_1K_2 + K_2N_2(1-\sigma)\} + K_0^2(1-\alpha_0)\{K_1(1-\sigma) + N_2 + K_2\sigma\}],$

where K_0, K_1, K_2 and K_b denote the bulk moduli of three constituent phases and porous skeleton, respectively.

Viscous cross-coupling coefficients are given by

$R_{11} = -\frac{\lambda_{22}\alpha_1^2}{\Delta}, \quad R_{12} = \frac{\lambda_{12}\alpha_1\alpha_2}{\Delta}, \quad R_{21} = \frac{\lambda_{21}\alpha_1\alpha_2}{\Delta}, \quad R_{22} = -\frac{\lambda_{11}\alpha_2^2}{\Delta},$

$\lambda_{11} = \left(\frac{1+\nu_1}{2}\right)b_1^*, \quad \lambda_{12} = \left(\frac{1-\nu_1}{2}\right)b_1^*, \quad \lambda_{21} = \left(\frac{1-\nu_2}{2}\right)b_2^*, \quad \lambda_{22} = \left(\frac{1+\nu_2}{2}\right)b_2^*,$

$\Delta = \lambda_{11}\lambda_{22} - \lambda_{12}\lambda_{21}, \quad \chi_1 = \sigma^\chi[1-(1-\sigma)^{\frac{n}{n-1}}]^{\frac{2(n-1)}{n}}, \quad \chi_2 = (1-\sigma)^\chi[1-\{1-(1-\sigma)^{\frac{n}{n-1}}\}^{\frac{n-1}{n}}]^2,$

$b_1^* = \chi_1/\eta_1, \quad b_2^* = \chi_2/\eta_2,$ where ν_j signifies the interfacial coupling parameter of fluid phases j (Ayub and Bentsen [33]). For an idealized channel flow, according to Ayub and Bentsen [33] $\nu_1 = \nu_2 = \nu = 1-\phi$ (ϕ being the porosity). η_1 and η_2 denote the viscosities of gas and liquid phases, respectively. The relative permeabilities χ_1, χ_2 for the flow of two pore-fluids are defined in comparison to the intrinsic permeability (χ_0) of the composite medium. The capillary pressure (p_c) is

due to the interfacial interactions between the two viscous pore-fluids. It varies with the fraction (σ) of gas or the fraction of liquid ($1-\sigma$) in twin-fluid mixture filling the pore space. The quantities m, n and χ are model parameters. These are obtained by fitting the experimental data on the p_c-σ and χ_j-σ relations, which are used in defining a_{ij}.

According to Lo et al. [19], inertial-coupling coefficients are given by

$A_{11} = \rho_1\alpha_1(1-\beta_s)$,

$A_{22} = \rho_2\alpha_2(1-\beta_s)$,

$A_{12} = A_{21} = -0.1\sqrt{\alpha_1\alpha_2\rho_1\rho_2\beta_s^2}$,

$\beta_s = \frac{\alpha_0}{2(\alpha_0-1)}$.

References

1. Biot MA (1956) Theory of propagation of elastic waves in a fluid saturated porous solid, I. Low-frequency range. *J Acoust Soc Am* 28: 168-178.
2. Biot MA (1956) Theory of propagation of elastic waves in a fluid saturated porous solid, II. Higher frequency range. *J Acoust Soc Am* 28: 179-191.
3. Biot MA (1962) Mechanics of deformation and acoustic propagation in porous media. *J Appl Phys* 33: 1482-1498.
4. Biot MA (1962) Generalized theory of acoustic propagation in porous dissipative media. *J Acoust Soc Am* 34: 1254-1264.
5. Brutsaert W (1964) The propagation of elastic waves in unconsolidated unsaturated granular mediums. *J Geophy Res* 69: 243-257.
6. Brutsaert W and Luthin JN (1964) The velocity of sound in sgass near the surface as a function of the moister content. *J Geophy Res* 69: 643-652.
7. Bedford A and Drumheller DS (1983) Theories of immiscible and structured mixtures. *Int J Eng Sci* 21: 863-960.
8. Garg SK and Nayfeh AH (1986) Compressional wave propagation in liquid and/or gas saturated elastic porous media. *J Appl Phys* 60: 3045-3055.
9. Berryman JG, Thigpen L, Chin RCY (1988) Bulk elastic wave propagation in partially saturated porous solids. *J Acoust Soc Am* 84: 360-373.
10. Santos JE, Corbero JM, et al. (1990) Static and dynamic behavior of a porous solid saturated by a two phase fluid. *J Acoust Soc Am* 87: 1428-1438.
11. Santos JE, Douglas J, Corbero JM, Lovera OM (1990) A theory for wave propagation in a porous medium saturated by a two phase fluid. *J Acoust Soc Am* 87: 1439-1448.
12. Corapcioglu MY and Tuncay K (1996) Propagation of waves in porous media, Advances in Porous Media, Vol. 3, M.Y. Corapcioglu ed., Elsevier, Amsterdam.
13. Tuncay K and Corapcioglu MY (1997) Wave propagation in poroelastic media saturated by two fluids. *J Appl Mech* 64: 313-319.

14. Wei C and Muraleetharan KK (2002) A continuum theory of porous media saturated by multiple immiscible fluids: I. Linear poroelasticity. *Int J Eng Sci* 40: 1807-1833.
15. Wei C and Muraleetharan KK (2002) A continuum theory of porous media saturated by multiple immiscible fluids: II. Lagrangian description and variational structure. *Int J of Eng Sci* 40: 1835-1854.
16. Hanyga A (2004) Two fluid porous flow in a single temperature approximation. *Int J Eng Sci* 42: 1521-1545.
17. Lu JF and Hanyga A (2005) Linear dynamic theory for porous media saturated by two immiscible fluids. *Int J Solids and Struct* 42: 2689-2709.
18. Lo WC (2008) Propagation and attenuation of Rayleigh waves in a semi-infinite unsaturated poroelastic medium. *Adv Water Resour* 31: 1399-1410.
19. Lo WC, Sposito G, Majer E (2005) Wave propagation through elastic porous media containing two immiscible fluids. *Water Resour Res* 41: 1-20.
20. Lo WC, Sposito G, Majer E (2009) Analytical decoupling of poroelasticity equations for acoustic-wave propagation and attenuation in a porous medium containing two immiscible fluids. *J Eng Math* 64: 219-235.
21. Lo WC, Sposito G, Majer E, et al. (2010) Motional modes of dilatational waves in elastic porous media containing two immiscible fluids. *Adv Water Resour* 33: 304-311.
22. Sharma MD and Kumar M (2011) Reflection of attenuated waves at the surface of a porous solid saturated with two immiscible viscous fluids. *Geophys J Int* 184: 371-384.
23. Kumar M and Kumari M (2014) Reflection of attenuated waves at the surface of a fractured porous solid saturated with two immiscible viscous fluids. *Latin Am J Solids Struct* 11: 1206-1237.
24. Sharma MD (2013) Effect of local fluid flow on reflection of plane elastic waves at the boundary of a double-porosity medium. *Adv Water Resour* 61: 62-73.
25. Sharma MD (2015) Constitutive relations for wave propagation in a double porosity solids. *Mech Mater* 91: 263-276.
26. Tomer SK and Goyal S (2013) Elastic waves in swelling porous media. *Transp Porous Media* 100: 39-68.
27. Carcione JM (2007) Wave Field in Real Media. Wave Propagation in Anisotropic, Anelastic, Porous and Electromagnetic Media. Pergamon, Amsterdam.
28. Lo WC, Yeh CL, Lee JW (2015) Effect of viscous cross coupling between two immiscible fluids on elastic wave propagation and attenuation in unsaturated porous media. *Adv Water Resour* 83: 207-222.
29. Borcherdt RD (2009) Viscoelastic waves in layered media. Cambridge University Press, New York.
30. Achenbach JD (1973) Wave Propagation in Elastic Solids, 1st Edition, North-Holland Publishing, Amsterdam.
31. Krebes ES (1983) The viscoelastic reflection/ transmission problem: two special cases. *Bull Seismol Soc Am* 73: 1673-1683.

32. Ainslie MA and Burns PW (1995) Energy-conserving reflection and transmission coefficients for a solid-solid boundary. *J Acoust Soc Am* 98: 2836-2840.

33. Ayub M and Bentsen RG (2005) Experimental testing of interfacial coupling in two-phase flow in porous media. *Pet Sci Technol* 23: 863-897.

AIMS Press